Polymer Journal, Vol. 29, No. 9, pp 722—732 (1997)

Theoretical and Experimental Analysis of Polymer Molecular Weight and Temperature Effects on the Dissolution Process of Polystyrene in Ethylbenzene

Bae Soo KONG, Yong Sung KWON,* and Dukjoon KIM†

Department of Chemical Engineering, Sung Kyun Kwan University, Suwon, Kyungki 440-746, Korea
**Department of Physics, Sung Kyun Kwan University, Suwon, Kyungki 440-746, Korea*

(Received February 12, 1997)

ABSTRACT: The effects of temperature and molecular weight on the polymer dissolution rate were investigated by comparison of the numerical simulation with the experimental observations. The Fickian diffusion equation was modified to predict the non-Fickian behavior by considering the temperature and concentration dependence of diffusion coefficient for moving (swelling) polymer films caused by solvent incorporation. The polymer dissolution process was predicted using the polymer chain disentanglement mechanism, founded on the reptation theory. The temperature and polymer molecular weight dependence of dissolution rate was measured using the laser interferometer technique. As results of simultaion and observations for the dissolution of polystyrenes in ethylbenzene, the dissolution rate increased with increasing temperature and decreasing polymer molecular weight and there was linear relationship between them in logarithmic scale. The experimentally determined values of exponent a and b which indicate the dependence strength of molecular weight and temperature on the dissolution rate were very similar to those theoretically estimated.

KEY WORDS Dissolution Rate / Reptation / Disentanglement / Non-Fickain Diffusion / Interferometer /

Nano- to micro- scaled thin polymer films have long been used in the corrosion protective or decorative applications. Its applications are recently extended to a variety of fields such as microelectronics fabrication, packaging systems for semi-conductor manufacture, membrane separation, and drug release systems. Thin polymer films used in the packaging and coating applications surrounded by environmental chemicals may cause deterioration of mechanical properties by swelling, cracking, and dissolution processes. In microelectronics fabrication, the use of thin polymer films for photoresists give a major role in the successful formation of lithographic image. The circuit accuracy is greatly affected by the development process in which the photoresist films are dissolved or swollen by appropriate solvents whether it is negative or positive system. When the solvent diffusion process is much slower than the dissolution process, the film swells too much to obtain the desired image resolution. On the other hand, when the swelling process is much faster than the dissolution process, a failure is resulted by over-development. Thus, the understanding of swelling and dissolution behavior is of a great importance to retain highly resolved lithographic image. Also, the effectiveness of the drug delivery system is mostly controlled by the swelling and dissolution properties of polymer matrix in contact with releasing medium of solvent. The higher rate of polymer swelling or dissolution, the higher drug releasing rate. The permselectivity of polymer membrane systems for liquid separation is significantly affected by the liquid-induced swelling or dissolution processes. The liquid to be separated may dissolve the short molecular chains resided in membrane materials or change the dimension of the membrane structure. It may deteriorate the final performance of membrane system.

As the application fields of the polymer swelling and dissolution processes are being expanded, the theoretical approaches on the analysis of these processes have been being widened. Founded on the reptation theory, Papanu *et al.*[1] reported that the dissolution rate was dependent on the polymer molecular weight and solvent concentration. In their report, however, the analysis of temperature effect on the dissolution process was omitted. Peppas *et al.*[2] analyzed the dissolution process of polystyrene in MEK using the polymer chain disentanglement mechanism with the concept of dissolution clock. They simulated the change of gel layer thickness during the dissolution process, and observed its existence by experiments. Other investigators[3-5] also tried to simulate dissolution processes with appropriate theories.

It is reported that the overall polymer dissolution process is microscopically divided into two successive processes—pure diffusion and pure dissolution. In this study, the overall dissolution process was simulated by polystyrene/ethylbenzene systems, by successive manipulation of diffusion and dissolution models, founded on the modiffed Fickian diffusion and the reptation theories, respectively. The molecular weight and temperature effect on the overall dissolution process was analyzed by comparison of the numerical simulation results with experimental data.

THEORY

Decrease in the film thickness is observed when the films of uncrosslinked polymers are in contact with good solvents. Such a polymer dissolution process is represented by the disentanglement of polymer chains after solvent penetration, accompanied by polymer swelling. Thus, a good representation of overall dissolution process needs at least two theoretical backgrounds—the one, the polymer swelling process caused by solvent incorporation, and the other, the pure polymer dissolution process caused by the chain disentanglements. The final process in relation with the overall dissolution process is the bulk transport process, which involves the movement of disentangled polymer chains from the polymer film phase to bulk solvent phase.

† To whom all correspondence should be addressed.

However, as this process is generally much faster than the two former processes, its effect is negligible in view of the kinetic analysis of overall dissolution process. When overall dissolution process continues, the film thickness changes successively as shown in Figure 1—increase by film swelling with solvent diffusion, followed by polymer chain disentanglement processes, and decrease by transport of disentangled polymer chains to bulk solvent. The theory and model corresponding to each process are represented as follows and overall process is simulated from their consecution.

Diffusion and Swelling Process

One dimensional diffusion process is assumed when the film thickness is much smaller than the width and length. The classical Fickian diffusion behavior in polymer systems characterized by the proportionality between the fractional mass uptake and square root of diffusion time is expressed by a well known Fick's law in which the constant diffusion rate is applied to the fixed boundary systems. In the actual diffusion process in the swelling polymer film, the diffusion rate is not constant, but varies with solvent concentration and temperature. This non-Fickian characteristics of solvent diffusion behavior in glassy polymers is possibly expressed by modification of the classical Fick's law. In this case, solvent diffusion process inside the moving (swelling) fiim is predicted, considering the concentration and temperature dependent diffusion coefficient. For one dimensional diffusion process as shown in Figure 2, the solvent mass flux inside the film is given by eq 1.

$$j_1 = -D_{12}(T, \phi_1)\frac{\partial \delta_1}{\partial x} = -D_0 f(T, \phi_1)\frac{\partial \phi_1}{\partial x} \qquad (1)$$

where x is the distance from the substrate surface to the film surface and D_{12}, the mutual diffusion coefficient can be expressed by the multiplication of D_0, an apparent diffusion coefficient and f, a function of ϕ_1, solvent volume fraction and T, temperature. In the present study f is defined in eq 19—22.

From the equation of continuity for a binary mixture with no chemical changes and negligible mixture velocity, the concentration profiles inside polymer film are obtained for increasing times with appropriate initial and boundary conditions.

$$\frac{\partial \phi_1}{\partial t} = -\frac{\partial j_1}{\partial x} \qquad (2)$$

$$\phi_1(x, 0) = 0 \qquad (3)$$

$$\phi_1(L^*, 0) = \phi_{1\,eq} \qquad (4)$$

$$\frac{\partial \phi_1(0, t)}{\partial x} = 0 \qquad (5)$$

Equation 3 implies that no solvent exists at the initial state. Equations 4 and 5 are two boundary conditions. Equation 4 represents that the concentration in the film surface is the same as the equilibrium concentration and eq 5 that the solvent mass flux is zero at the interface between film and substrate, respectively.

The equilibrium solvent concentration of $\phi_{1\,eq}(=1-\phi_{2\,eq})$ at the film surface can be obtained from eq 6 provided by the Flory–Huggins theory.[6] The solvent chemical potential difference between the polymer solution and bulk solvent is zero at equilibrium condition.

$$\mu_1 - \mu_1^0 = RT[\ln(1-\phi_{2\,eq}) + (1-1/x_p)\phi_{2\,eq} + \chi_1\phi_{2\,eq}^2 + V_1\rho_2(4/M_e - 1/M)(2\phi_{2\,eq}^{1/3} - \phi_{2\,eq})] = 0 \qquad (6)$$

where R is gas constant, V_1 solvent specific volume, x_p degree of polymerization, M_e the molecular weight between entanglements, ρ_2 polymer density, and χ_1 is polymer–solvent interaction parameter.

As the polymer film is swollen by solvent penetration, the moving boundary position should be considered. The relationship between the material coordinate which is based on the deformed film state and the fixed coordinate which is based on the undeformed state is given by the solvent-induced deformation strain tensor, ε_{XX}, under the assumption of one dimensional diffusion process.

$$dx = (1+\varepsilon_{XX})dX = \frac{1}{\phi_2}dX \qquad (7)$$

Dissolution Process

Glass transition temperature of polymer film is decreasing with increasing solvent concentration by plas-

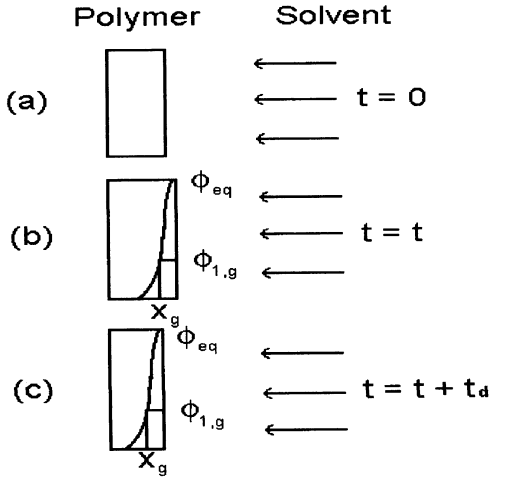

Figure 1. Schematic representations of a one-dimensional solvent diffusion and polymer dissolution process: (a) Initial position of polymer/solvent contact system. (b) Moving positions of the solvent-polymer and gel/glassy interfaces by swelling induced by solvent penetration, (c) Moving positions of the solvent/polymer and gel/glassy interfaces by dissolution after a time period of t_d.

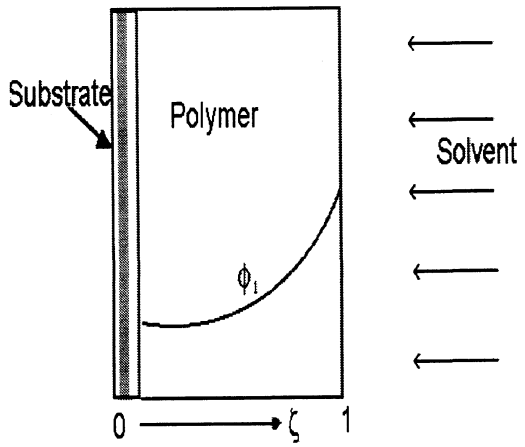

Figure 2. Representation of concentration profiles and boundary positions for one dimensional solvent diffusion in thin polymer film.

ticizing effect. The different solvent concentration at different film position during diffusion and dissolution processes results in the position dependent glass transition temperature (=local glass transition temperature) inside the film. In this study, when the local glass transition temperature is the same as the experimental temperature, the corresponding solvent concentration is termed as the gel concentration. When the solvent concentration at certain film position reaches the gel concentration, the glass to rubber transition occurs and the disentanglement process starts because the short range diffusive motion of polymer chain segments begins to exist. This phenomenon can be well expressed by the reptation theory.

In the reptation theory,[7] the chain disentanglement process is described by the snake-like movement of polymer chains through the characteristic tube whose diameter is constrained by multiple chain entanglement points. The time to escape this tube with a finite length by reptational motion is characterized by the disentanglement time, or dissolution time, t_d. It means that the dissolution process, or disentanglement process starts when the local solvent concentration reaches the gel concentration, and continues for t_d to escape through the hypothetical tube whose length is characterized by the molecular weight of polymer. After disentanglement time of t_d, the disentangled polymer chains are transported to the bulk solvent in negligible time scale.

The disentanglement rate in reptation theory is given by the ratio of radius of gyration to the characteristic tube diffusion coefficient and is a function of polymer molecular weight and solvent concentration. The resulting disentanglement time is well reported as in eq 8 for good solvents[7] and may be extended to general solvents as in eq 9 by replacing the exponent values of 3 and 1.5 with a and b.

$$t_R = k(\eta_{sol}/T)M^{3.0}\phi_2^{1.5} \tag{8}$$

$$t_d = k'(\eta_{sol}/T)M^a\phi_{2\,eq}^b \tag{9}$$

where k and k' are coefficients.

Normalization

To solve eq 1—5 and 9 with relative ease, the variables such as t, ϕ_1, x, and t_d can be normalized as shown in eq 10—12, based on D_0, the apparent diffusion coefficient, L^*, the initial thickness of polymer film and $\phi_{1\,eq}$, the equilibrium solvent volume fraction.

$$\tau = \frac{D_0 t}{L^{*2}}, \qquad \tau_d = \frac{D_0 t_d}{L^{*2}} \tag{10}$$

$$\eta = \frac{x}{L^*} \tag{11}$$

$$\bar{\phi}_1 = \frac{\phi_1}{\phi_{1\,eq}} \tag{12}$$

Then, eq 2 with initial and boundary conditions 3, 4, and 5 are changed to the following normalized expressions:

$$\frac{\partial \bar{\phi}_1}{\partial \tau} = f(\bar{\phi}_1, T)\frac{\partial^2 \bar{\phi}_1}{\partial \eta^2} \tag{13}$$

$$\bar{\phi}_1(\eta, 0) = 0 \tag{14}$$

$$\bar{\phi}_1(0, \tau) = 1 \tag{15}$$

$$\frac{d\bar{\phi}_1(\eta=0, \tau)}{d\eta} = 0 \tag{16}$$

The fractional solvent mass uptake during the dissolution process is given by eq 17, as it can be determined by the integration of fractional solvent volume fraction with respect to the residual film thickness.

$$\frac{M_t}{M_\infty} = \int_{\eta=0}^{\eta=\eta_s} \bar{\phi}_1 d\eta \tag{17}$$

Physical Properties of Polystyrene/Ethylbenzene Systems

In order to simulate the dissolution behavior of polystyrene in ethylbenzene, all the physical properties involved in the dissolution process should be addressed. Many physical properties involved in eq 6, 9, and 13 were possibly obtained from literature.

The interaction parameter of polystyrene/ethylbenzene, χ_1, was correlated with temperature as in eq 18 from the best curve fitting to the experimental results.[8]

$$\chi_1(T) = \frac{27.3231}{(T-273.15)} - 0.007692 \tag{18}$$

where T is absolute temperature.

The concentration and temperature dependence of self-diffusion coefficient of ethylbenzene is well described by the Vrentas and Duda's hole free volume theory[9] as in eq 19 and 20.

$$D_1 = D_0 \exp[(-E/RT)] \exp[-\gamma(\omega_1 V_1^* + \omega_2 \xi V_2^*)/V_{FH}] \tag{19}$$

$$V_{FH}/\gamma = (K_{11}/\gamma)\omega_1(K_{21} + T - T_{g1}) + (K_{12} + T - T_{g2}) \tag{20}$$

where ω_1 and ω_2 are weight fractions of solvent and polymer, respectively, and can be transformed to volume fractions according to eq 21.

$$\phi_1 = 1/[1 + (1/\omega_1) - 1)(\rho_1/\rho_2)] \tag{21}$$

In polystyrene/ethylbenzene system, all values of parameters in eq 19 and 20 were provided by Vrentas and Chu.[10] (refer to Table I).

The mutual diffusion coefficient is correlated with the self-diffusion coefficient by the Flory–Huggins' thermodynamic theory.

Table I. Free volume parameters for the polystyrene/ethylbenzene system

Parameter	Values
ξ_i	0.58
D_0/cm^2 s^{-1}	5.33×10^{-4}
E/kcal g mol^{-1}	0.694
$\hat{V}_1$/cm^3 g^{-1}	0.946
$\hat{V}_2$/cm^3 g^{-1}	0.850
K_{11}/γ (cm^3 g^{-1} K)	1.49×10^{-3}
K_{12}/γ (cm^3 g^{-1} K)	5.82×10^{-4}
$K_{21} - T_{g1}$/K	−84.4
$K_{22} - T_{g2}$/K	−327

$$D_{12}=D_1\phi_2\left[\phi_2(1-2\chi_1\phi_1)+\frac{M_1\hat{\phi}_1}{\bar{M}_c\phi_2}\phi_1\left(\frac{1}{2}-\frac{1}{3}\phi_2^{-(2/3)}\right)\right] \quad (22)$$

where $\bar{M}_c$ is the average molecular weight between consecutive crosslinks. The values of specific volume of ethylbenzene and polystyrene are 1.154 and 0.9280 $cm^3\,g^{-1}$, respectively.

Below glass transition temperature, eq 19 has been replaced with eq 23 with parameter λ indicating the fractional free volume decrease in glass region.[11] The value of λ has been set to be 0 in our study because the fractional free volume is almost constant below T_g.

$$\ln\left[\frac{D_{12}(T)}{D_{12}(T_{g2})}\right]=\frac{\gamma\hat{V}_2\xi}{K_{12}}\cdot\frac{T-T_{g2}}{K_{22}[(K_{22}/\lambda)+T-T_{g2}]} \quad (23)$$

Figure 4 represents the concentration dependence of the mutual diffusion coefficient for varying temperatures. The diffusion coefficient has maximum values around the solvent volume fractions ranging from 0.4 to 0.6. Below gel concentration, the diffusion coefficient has constant values for all temperatures of interest.

Glass transition temperature of polystyrene decreases with solvent concentration. The relationship between T_g and ϕ_1 is shown in eq 24.[12]

$$\phi_{1,g}(T)=-2.228\times10^{-3}T_g+8.3118\times10^{-1} \quad (24)$$

The entanglement molecular weight, M_e, was reported to be related with the critical molecular weight of M_c as in eq 25.[13] In the present analysis, a typical critical molecular weight of 38000 was incorporated.[14]

$$M_2\sim M_c/2 \quad (25)$$

Viscosity of ethylbenzene is correlated with temperature by eq 26.[15]

$$\eta_{sol}\sim T^{-3.4} \quad (26)$$

Numerical Solution

Equations 13 to 17 were solved by appropriate numerical methods.[16,17] The partial differential eq 13 with the initial and boundary conditions 13, 14, and 15 were solved using the Crank Nicholson's finite difference method. The integral equation 17 was solved using the 15 point Gauss–Legendre method.

The numerical solution was proceeded as follows: i) the local concentration inside the film was determined from eq 13 for each time increment; ii) if the local concentration at certain time reaches the gel concentration in which the corresponding local glass transition temperature is the same as the operation temperature, the clock is set to be zero; iii) when the clock is the same as the disentanglement time, t_d, which is determined by eq 9, the film surface moves to this position. In this case t_d may change continuously from maximum to minimum as the local solvent concentration increases for time increment; iv) the equilibrium solvent concentration at the polymer/solvent interface is recalculated from eq 6; v) (i) to (iv) are repeated until the bare substrate confronts to the bulk solvent.

In the procedures from i) to v), three important quantities are calculated. The first one is the variation of local diffusion coefficient inside film during dissolution process, as the diffusion coefficient is a function of concentration in isothermal process. The second is the local solvent concentration calculated from eq 13, and the third is the variation of film thickness for dissolution time. In this study two points were tried to be verified. The one is whether the actual dissolution process is well described by the reptation theory, and the other is whether the exponent values of a and b experimentally determined are in accordance with those represented by reptation theory.

EXPERIMENTAL

Materials

Polystyrene/ethylbenzene systems were chosen in this study, as polystyrene, a typical amorphous polymer, is one of the widely used ones and relatively many physical data are available for this system.

Polystyrene samples of molecular weights of 45000, 190000, and 280000 g g mol^{-1} were purchased from Scientific Polymer Products, and ethylbenzene was from Junsei Chemical Company. The refractive indices of polystyrene and ethylbenzene were 1.59 and 1.496, respectively. Toluene was used to dissolve the polystyrene in preparation of thin film on the silicone substrate.

Interferometer Set-up

The film thickness change during the dissolution process was measured by interferometer method. Interferometer apparatus was composed of helium-neon laser (model 1134p, Uniphase, U.S.A.) of wavelength of 632 nm, focusing lens, display multimeter (Fluke 45, Fluke Co.), photodiode (model S2386-8K, Hamamatsu, U.S.A.), pin hole, and temperature controlled dissolution chamber as shown in Figure 3. Measurements were performed at temperatures of 20, 30, 40, 50, 60, 70, and 90°C in the black box to minimize the noise caused by environmental light. Temperature was controlled in the

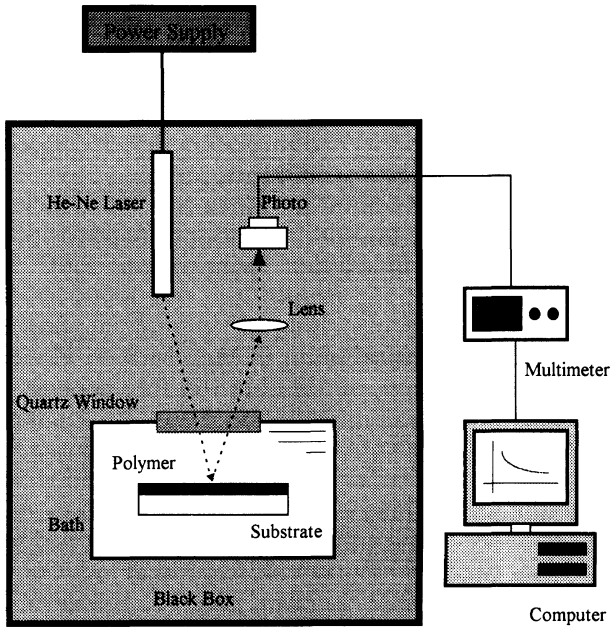

Figure 3. Schematic apparatus for film thickness measurement.

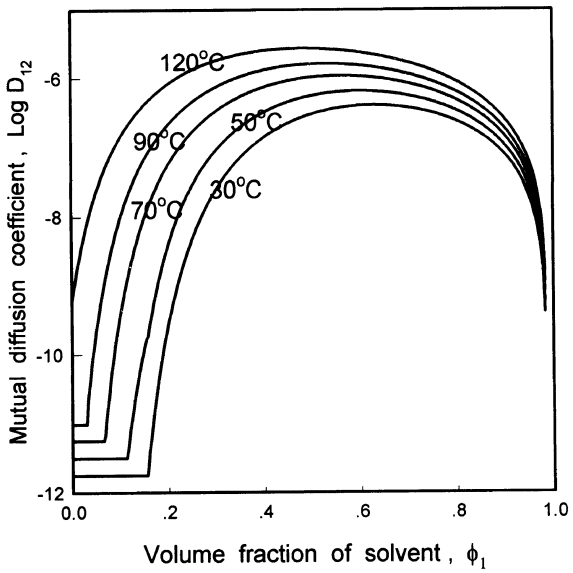

Figure 4. Concentration dependence of the mutual diffusion coefficient for polystyrene/ethylbenzene systems at temperatures of 120, 90, 70, 50, and 30°C.

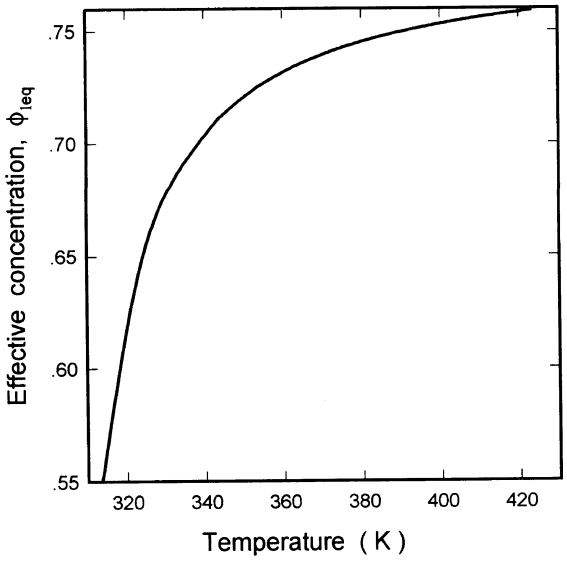

Figure 5. Equilibrium volume fraction of ethylbenzene in the polystyrene/ethylbenzene system as a function of temperature.

accuracy of ± 1°C. Optical lens was used to expand the interference patterns caused by the optical path length difference between the light reflected from the film surface and that reflected from the substrate surface. The interference pattern detected by a photodiode was digitalized by a multimeter. The digitalized data were transferred to a personal computer where the data were analyzed. A Bias circuit was constructed on the photodiode detector to increase the optical gain. The physics and mathematics related in measuring the film thickness by this interferometer method was well described in other reports.[18-20]

Measurement of Film Thickness Change

Polystyrene samples dissolved in toluene (10 wt%) were spin coated on the silicon substrate using a spin coater (model 1-EC101DT-R485, Headway Research Inc., U.S.A.). The coated film on the substrate was dried in vacuum oven at 160°C for 12 hours. The thickness of solution-free polystyrene film was measured using micrometer (model MI20-25, Mitutoyo, Japan). The film thickness of 1 to 2 μm was controlled by changing the solution concentration and revolution time and speed of spin coater from 500 to 3000 rpm.

The experiments for the measurement of film thickness change during the dissolution process were performed as follows: (i) the dissolution chamber was filled with ethylbenzene and the temperature was adjusted by a heating coil with controller; (ii) during the time for stabilization of temperature in the chamber, the bare substrate was placed on the holder in the chamber; (iii) the laser power was turned on to adjust the beam pass from laser to photodiode; (iv) as the laser power was unstable in the initial state, the measurements were started at least 1 hour later; (v) after the stabilization of the chamber temperature and the laser power had been checked, the bare substrate was replaced with the film coated substrate and the beam pass was realigned; (vi) the measurement was started and continued until no polymer film existed on the substrate; (vii) (i) to (vi) were performed for polystyrene samples of different molecular weights at varying temperatures.

RESULTS AND DISCUSSION

Diffusion and Swelling Behavior

In the dissolution process of polystyrene in ethylbenzene with the physical properties provided by eq 18 to 26, the solvent concentration profiles inside film and dissolution rate were determined by the numerical solution methods mentioned in THEORY. In this calculation, the time interval was chosen as 1×10^{-5} s and the local film position was obtained by dividing the total film thickness by 100 into the direction of solvent penetration.

With the proposed physical properties of polystyrene/ethylbenzene, the temperature dependence of the equilibrium concentration at the polymer film/solvent interface has been determined from eq 6 and their results are illustrated in Figure 5. As temperature increased, the equilibrium solvent fraction increased because the polymer/solvent interaction parameter decreased with increasing temperature.

(a), (b), and (c) of Figure 6 show the variation of local concentrations inside polymer film during dissolution processes at 50, 70, and 90°C. Each curve represents the concentration distribution at each dissolution time. The concentration at the film surface reaches the equilibrium concentration when polymer film contacts with the bulk solvent, and the solvent penetrates into the film with time increment, resulting in continuous concentration distributions as shown in Figure 6. Once a certain local concentration was the same as the gel concentration, the disentanglement process started. After duration of t_d, the gel sections which had higher solvent concentrations than the gel concentration were dissolved, and a new film surface confronted to the bulk solvent. These processes continued repeatedly until no film was observed on the film. The equilibrium solvent concentration and the dissolution rate increased with increasing temperatures.

The concentration profiles inside the undissolved film

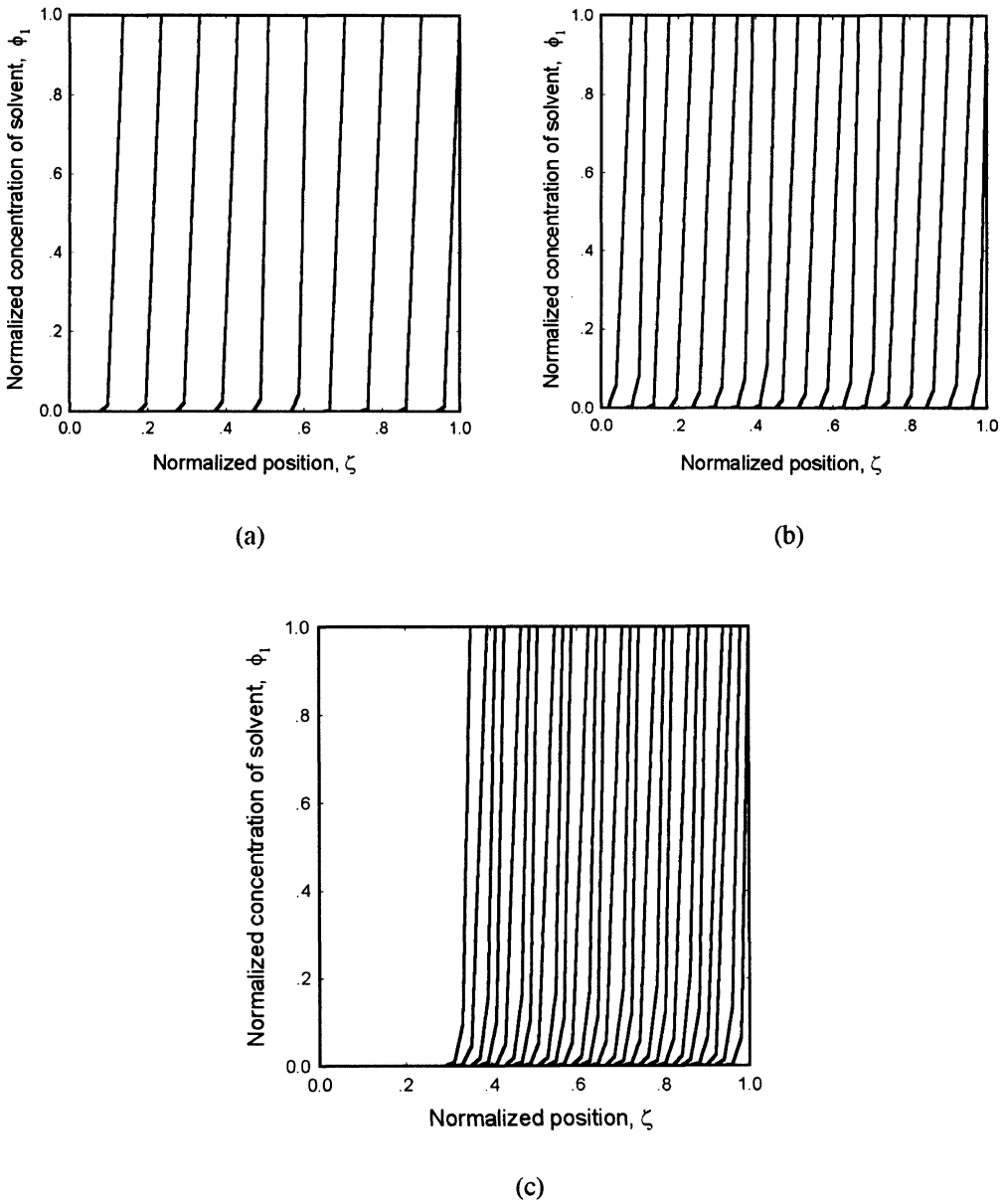

Figure 6. Normalized solvent concentration as a function of normalized position during polymer (MW = 400000 g gmol^{-1}) dissolution processes at (a) 90, (b) 70, (c) 50°C. Each curve represents the profile of local diffusion coefficient at the normalized time interval of 1.7×10^4. The dissolution parameters chosen were $a=2$, $b=6$, and $k'=0.2 \times 10^{-18}$, respectively.

led to distributions of diffusion coefficients. Each local diffusion coefficient corresponding to each local concentration is shown in Figure 7. The diffusion coefficient had the values ranging from 10^{-12} to 10^{-5} cm^2 s^{-1}, and the maximum value appeared not at the film surface itself, but inside the film near the film surface, as the concentration dependence of diffusion coefficient was not linear, but was maximized around the solvent concentrations of 0.6. The constant diffusion coefficient near the substrate surface indicates that the local concentrations in this region are lower than the gel concentration. Values of diffusion coefficients at the film surfaces increased with increasing temperatures.

Figure 8 shows the fractional mass of solvent absorbed in the undissolved film during the dissolution process. The increase in the fractional mass uptake with dissolution time was caused by the decrease of the thickness of glassy region. The fluctuation of local solvent mass uptake was caused by the repeating processes of swelling and dissolution. During the diffusion and disentanglement processes the solvent was being absorbed, but after t_d the local film position containing high solvent concentrations was detached from the bulk film and a new film/solvent interface was formed.

Molecular Weight and Temperature Effects on Dissolution Rate

Figure 9 shows the variation of film thickness during the dissolution process. The behavior of film thickness is given by two curves, the upper of which shows the film/solvent interface and the lower of which shows the glass/rubber transition position. The distance between the upper and lower curves is the thickness of gel layer. The reason there is a discontinuity in each curve is that the time duration of t_d is needed for the polymer chains to disentangle after the local solvent concentration reaches the gel concentration. During the disentanglement process, only solvent diffusion, accompanied by

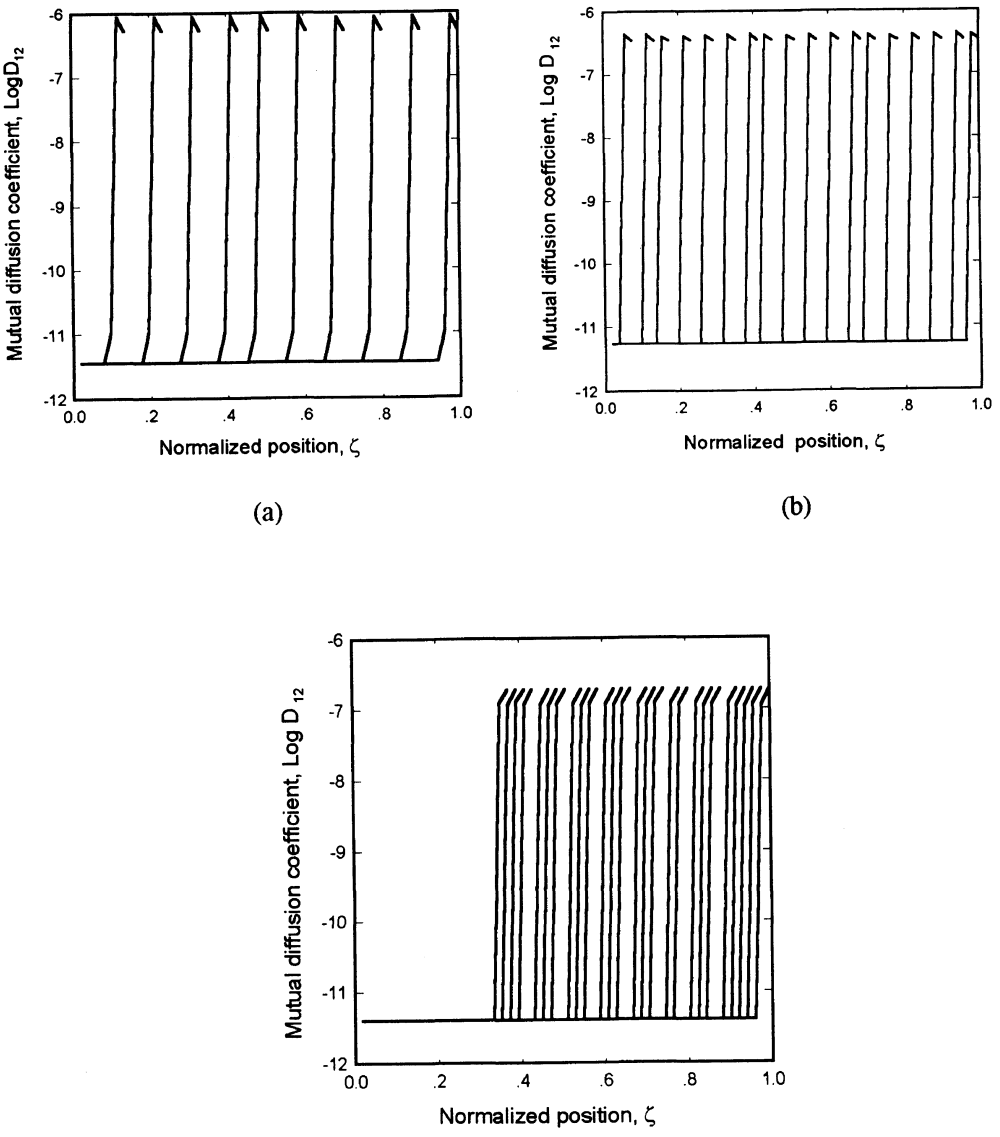

Figure 7. Mutual diffusion coefficient of polystyrene/ethylbenzene system as a function of normalized position during polymer dissolution processes at (a) 90, (b) 70, and (c) 50°C. Each curve represents the profile of local diffusion coefficient at the normalized time interval of 1.7×10^4. The dissolution parameters chosen were $a=2$, $b=6$, and $k'=0.2 \times 10^{-18}$, respectively.

film swelling process proceeded. The average thickness change represented by dotted curve is obtained by the linear regression of discontinuous values of thickness. As shown in Figure 9(a), the overall dissolution time increases with polymer molecular weight. This is explained by eq 9 in which the dissolution time increases with molecular weight with power exponent values of a. The gel layer thickness also increased with polymer molecular weight for the same reason.

Another factor to affect the dissolution rate is temperature. As shown in Figure 9(b), the film thickness linearly decreased with dissolution time except the initial and final stages. The increasing temperature resulted in the increasing dissolution rate. The temperature effect on the gel layer thickness was not severe in this experimental temperature range, being different from the molecular weight effect. The temperature effect on the overall dissolution rate arised from the two factors. The first is from the temperature dependence of mutual diffusion coefficient. The higher temperature led to the higher diffusion rate, and it resulted in the less time to reach the gel concentration. The second is from the temperature dependence of dissolution time as expressed in eq 9, in which the solvent viscosity and polymer concentration are a function of temperature.

To analyze the molecular weight and temperature dependence of the dissolution rate, the simulation results were compared with the experimental data. Theoretical dissolution rate is scaled by eq 27.

$$R_d \sim \frac{\delta}{t_d} \tag{27}$$

For isothermal conditions the molecular weight dependence is given by eq 28, as the gel layer thickness is scaled by eq 30 which is originated from eq 29 when the diffusion coefficient is not significantly affected by polymer molecular weight.

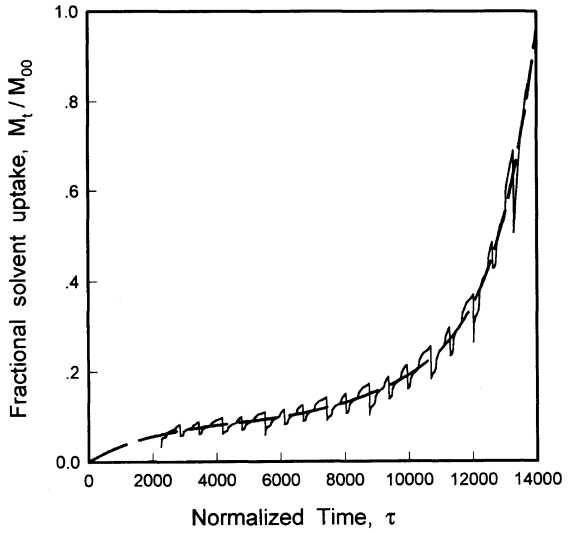

Figure 8. Fractional ethylbenzene uptake in polystyrene (MW = 400000 g gmol^{-1}) during dissolution process at 90°C when the dissolution parameters chosen were $a=2$, $b=6$, and $k'=0.2\times10^{-18}$, respectively. The dashed curve indicates the continuous profile after regression.

$$R_d \sim M^{-(a/2)} \tag{28}$$

$$t_d \sim \delta^2/D_{12} \tag{29}$$

$$\delta \sim M^{a/2} \tag{30}$$

As shown in Figure 10, the molecular weight dependence of dissolution rate is linear in logarithmic scale. The slope value of -1.4 indicates the exponent value a in eq 9 is 2.8.

Theoretical analysis of temperature effect on the overall dissolution rate is relatively complicated, as several parameters involved in dissolution equations such as D_{12}, χ_1, ϕ_1, and η_s are a function of temperature. Thus, in this analysis the temperature dependence of gel layer thickness was obtained from the final simulation results. The fact in Figure 9(b) that the gel layer thickness was negligibly affected by variation of temperature possibly led to the following correlations:

$$R_d \sim \frac{1}{t_d} \tag{31}$$

For a fixed molecular weight eq 9 is simplified to eq 32.

$$t_d \sim \frac{\eta_{sol}}{T}\phi_{2\,eq}^{b} \tag{32}$$

From Figure 5 $\phi_{2\,eq}$ is correlated with T as in eq 33.

$$\phi_{2\,eq} \sim T^{-1.3} \tag{33}$$

Incorporation of eq 26, 33, and 32 to eq 31 resulted in the final scaling correlation of dissolution rate and temperature.

$$R_d \sim T^{4.4+1.3b} \tag{34}$$

The temperature dependence of dissolution rate experimentally observed is shown in Figure 11. The linear regression of dissolution rate with respect to the temperature in logarithmic scale gave the slope values of 6.7, 6.8, and 6.01 for different polymer molecular weights of 45000, 190000, and 280000 g g mol^{-1}, respectively. This means the exponent value of b in eq 9 could be chosen as 1.5 ± 0.3. The exponential dependence of molecular weight and temperature on the dissolution rate experimentally analyzed was very similar to that predicted from the reptation theory.

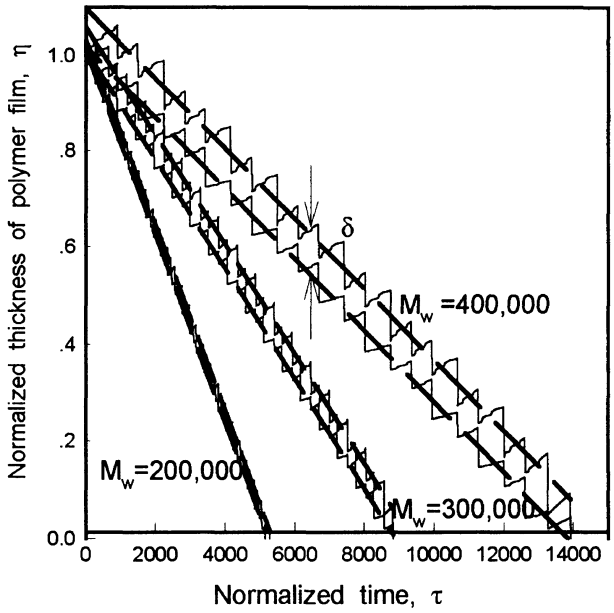

(a)

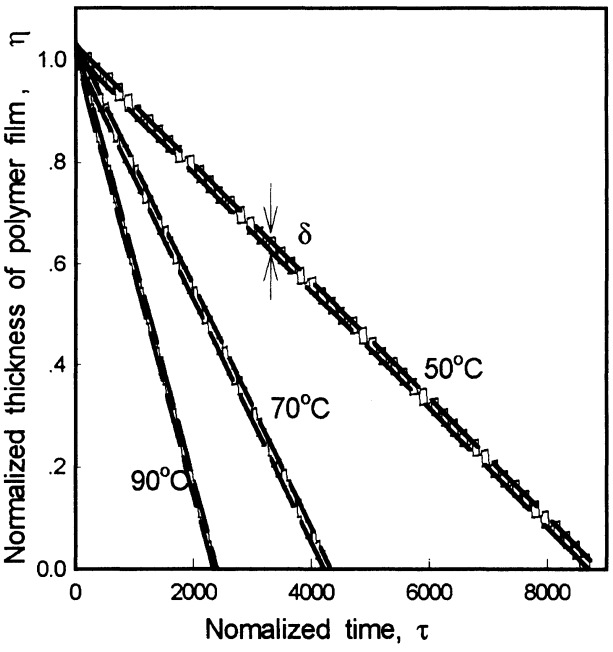

(b)

Figure 9. Normalized thickness of polymer film as a function of normalized dissolution time (a) for varying polymer molecular weights of 200000, 300000, and 400000 g g mol^{-1} at 30°C, and (b) for varying temperatures of 90, 70, and 50°C for MW = 400000 g g mol^{-1}. For each representation, the upper curve represents boundary between polymer and bulk solvent and the lower curve the boundary between glass and gel. The dashed curve corresponding to each boundary indicates the continuous profile after linear regression. The dissolution parameters chosen were $a=2$, $b=6$, and $k=0.2\times10^{-18}$, respectively.

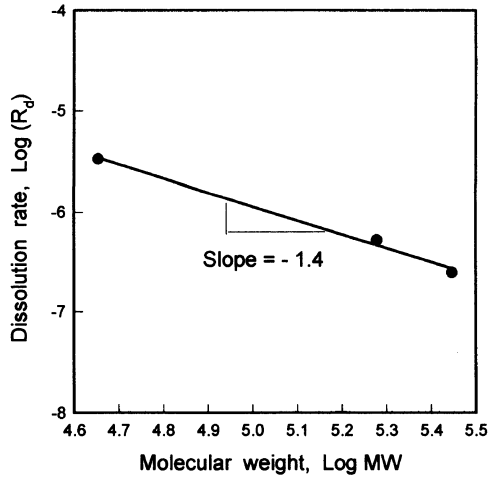

Figure 10. Polymer molecular weight effect on the dissolution rate at 90°C.

Even the molecular weight and temperature dependence of dissolution rate was determined and was very similar between the theoretical and experimental approaches, the dissolution coefficient, k', in eq 9 has not been determined. In order to determine the value of k' with the predetermined values of exponent, a and b, the best fitting of experimental data was performed. In Figure 12, the temperature dependence of experimental data was fitted with the simulation results for varying k' values. The k' values did not affect the temperature dependence (slope), but greatly affected the overall dissolution rate. The best fitting to experimental data gave the k' value of 3×10^4.

CONCLUSIONS

A model was developed to simulate the dissolution behavior of thin glassy polymer film in solvent. Non-

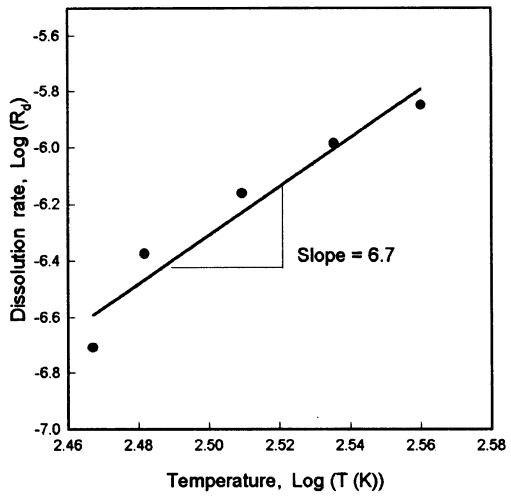

(a)

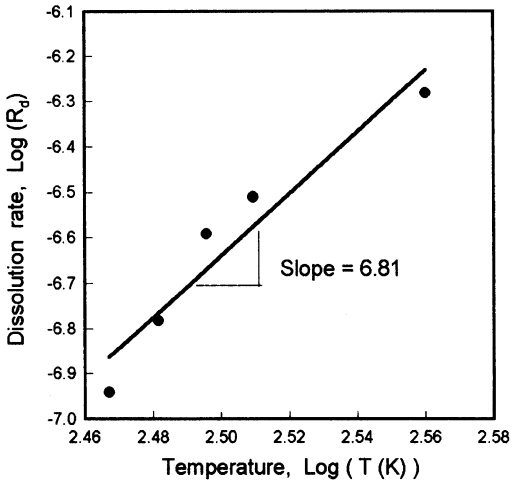

(b)

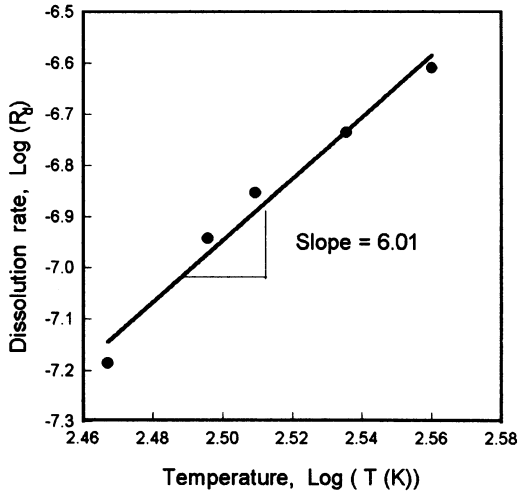

(c)

Figure 11. Temperature effect on the dissolution rate for polymer molecular weights of (a) 45000, (b) 190000, and (c) 280000 g g mol^{-1}, respectively.

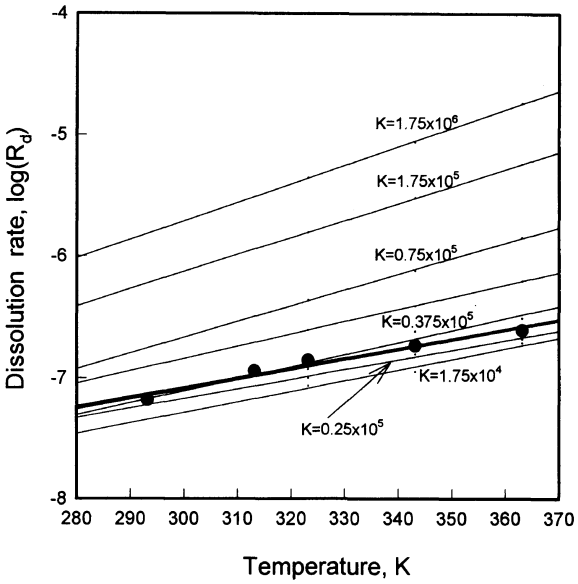

Figure 12. Temperature effect on the dissolution rate of polymer (MW = 280000 g g mol^{-1}) for varying k' values from 1.75×10^4 (bottom) to 1.75×10^6 (top) with $a = 2.8$ and $b = 1.6$. Circles indicate the experimental data.

Fickian characteristics of solvent diffusion behavior in glassy polymers was described by a modification of Fickian diffusion theory in which the solvent concentration and temperature dependence of diffusion coefficient is involved for the moving boundary systems induced by polymer swelling and dissolution processes. Concentration and temperature dependence of diffusion coefficient was obtained from the Vrentas–Duda's free volume theory. The reptation theory was adapted to describe the pure dissolution process, as it is described by the chain disentanglement process from the initially chain entangled state by solvent penetration. As results of simulation, the dissolution rates decreased with increasing molecular weight and decreasing temperature and there were linear relationships between each other in logarithmic scale. The gel thickness increased with increasing molecular weight and decreasing temperature as it took more time to reach the gel concentration and to disentangle the polymer chains. The molecular weight and temperature dependence of dissolution rate theoretically predicted was investigated with the experimental observation. The film thickness change during the dissolution process was measured using the interferometric technique. The resulting values of exponent a and b which are indications of dependence of molecular weight and temperature on the dissolution rate are very similar to those for the dissolution process in good solvent. From the best curve fitting to the experimental data with the simulated behavior the dissolution coefficient, k', was determoned as 3×10^4.

Acknowledgment. This work was supported by the Korea Science and Engineering Foundation Grant 951-1101-045-2.

LIST OF SYMBOLS

Symbol: name [Unit]
D_0, constant pre-exponential factor [cm^2 s]$^{-1}$
D_1, self-diffusion coefficient [cm^2 s^{-1}]
D_{12}, mutual diffusion coefficient [cm^2 s^{-1}]
E, the energy per mole that a molecule needs to overcome attractive force which hold it to its neighbors. [kcal g mol^{-1})
j_s, mass flux of solvent in polymer film [g cm^{-2} s]
K_{11}, free volume parameter for the solvent [cm^3 g^{-1}K]
K_{21}, free volume parameter for the solvent [cm^3 g^{-1} K]
K_{12}, free volume parameter for the polymer [cm^3 g^{-1} K]
K_{22}, free volume parameter for the polymer [cm^3 g^{-1} K]
k, constant
k', constant
L^*, initial film thickness [μm]
M, molecular weight of polymer [g g mol^{-1}]
M_c, critical molecular weight [g g mol^{-1}]
M_e, molecular weight between entanglement chain [g/entanglement unit]
M_t, mass uptake of solvent at time t [g]
M_∞, mass uptake of solvent after infinite time [g]
$\bar{M}_c$, average molecular weight between crossinks
R, gas constant [1.987 cal mol^{-1} K]
R_d, disentanglement rate [cm s^{-1}]
T, temperature [K]
T_{g2}, glass transition temperature of polymer [K]
t, time [s]
t_d, disentanglement time [s]
t_R, reptation time [s]
V_1, molar volume of solvent [cm^3 mol^{-1}]
$\hat{V}_1^*$, specific critical hole-free volume of solvent required for a jump [cm^3 g^{-1}]
$\hat{V}_{FH}$, average specific hole free volume per gram of mixture [cm^3 g^{-1}]
X, undeformed coordinate
x, deformed coordinate
α, constant
β, constant
γ, overlap factor which is introduced because the same free volume is available to more than one molecule
δ, gel thickness
ζ, dimensionless boundary condition based on the undeformed coordinate
η, dimensionless position
η_s, dimensionless position at polymer surface
η_{sol}, solvent viscosity [g cm^{-1} s]
ξ_i, the ratio of the critical molar volume of the solvent jumping unit to the critical molar volume of the polymer jumping unit
μ_1, chemical potential of solvent in solution
μ_1^0, chemical potential of solvent in the pure liquid.
ρ_1, density of solvent [g cm^{-3}]
ρ_2, density of polymer [g cm^{-3}]
τ, dimensionless time
τ_d, dimensionless disentanglement time
ϕ_1, solvent volume fraction
$\phi_{1\,eq}$, effective solvent fraction at surface
$\phi_{1,g}$, gel concentration of solvent
χ_1, polymer/solvent interaction parameter
ω_1, solvent mass fraction
ω_2, polymer mass fraction

REFERENCES

1. J. S. Papanu, D. S. Soane, and A. T. Bell, *J. Appl. Polym. Sci.*, **38**, 859 (1989).

2. N. A. Peppas, J. C. Wu, and E. D. Meerwall, *Macromolecules*, **27**, 5626 (1994).
3. H.-R. Lee and Y.-D. Lee, *Chem. Eng. Sci.*, **46**, 1771 (1991).
4. M. F. Herman and S. F. Edwards, *Macromolecules*, **23**, 3662 (1990).
5. L. Schlegel and W. Schnabel, *J. Appl. Polym. Sci.*, **41**, 1797 (1990).
6. P. J. Flory, "Principles of Polymer Chemistry," Cornell University, Ithaca and London, 1971, pp 495—594.
7. P-G. de Gennes, "Scalling Concepts in Polymer Physics," Cornell University Press, Ithaca and London, 1979, pp 219–230.
8. B. Carnahan, H. A. Luther, and J. O. Wilkes, "Applied Numerical Methods," Wiley, New York, N.Y., 1989, Chapter 7.
9. W. H. Press, B. P. Flannery, S. A. Teukolsky, and W. T. Vetterling, "Numerical Recipes in C," Cambridge University Press, New York, N.Y., 1988.
10. P. D. Krasicky, R. J. Groele, J. A. Jubinsky, and F. Rodriguez, *Polym. Eng. Sci.*, **27**, 282 (1987).
11. F. Rodriguez, P. D. Krasicky, and R. J. Groele, *Sol. Stat. Technol.*, **28**, 125 (1985).
12. P. D. Krasicky, R. J. Groele, and F. Rodriguez, *Chem. Eng. Comm.*, **54**, 279 (1987).
13. J. Brandrup and E. H. Immergut, Ed., "Polymer Handbook," 2nd ed, Wiley, New York, N.Y., 1975, Section VII.
14. J. S. Vrentas, J. L. Duda, H.-C. Ling, and A.-C. Hou, *J. Polym. Sci., Polym. Phys. Ed.*, **23**, 289 (1985).
15. J. S. Vrentas and C.-H. Chu, *J. Appl. Polym. Sci.*, **34**, 587 (1987).
16. J. S. Vrentas, J. L. Duda, and H. T. Liu, *J. Appl. Polym. Sci.*, **25**, 1297 (1980).
17. J. Klein, "Encyclopedia of Polymer Science and Engineering," 2nd ed, Wiley, New York, N.Y., 1987, Vol. 5.
18. W. W. Graessley, *Adv. Polym. Sci.*, **16**, 1 (1974).
19. L. H. Sperling, "Introduction to Physical Polymer Science," 2nd ed, Wiley, New York, N.Y., 1992, p 482.
20. D. R. Lide, "Handbook of Organic Solvent," CRC Press, Boca Raton, 1995, p 211.